Atmospheric Environment 248 (2021) 118180

Contents lists available at ScienceDirect

Atmospheric Environment

journal homepage: http://www.elsevier.com/locate/atmosenv

Diurnal patterns in ambient $PM_{2.5}$ exposure over India using MERRA-2 reanalysis data

Kunal Bali[a], Sagnik Dey[a,b,*], Dilip Ganguly[a]

[a] Centre for Atmospheric Sciences, Indian Institute of Technology Delhi, Hauz Khas, New Delhi, India
[b] Centre of Excellence for Research on Clean Air, Indian Institute of Technology Delhi, Hauz Khas, New Delhi, India

HIGHLIGHT

- Diurnal pattern of ambient $PM_{2.5}$ is examined over India using MERRA-2 reanalysis data
- MERRA-2 data is calibrated using reference grade monitor data
- Diurnal amplitude exceeds 30 µg m^{-3} over large part of the country
- Annual increasing trend is strongly governed by the trend in Oct–Feb
- A declining planetary boundary layer height contributes to the rise in $PM_{2.5}$ in these months

GRAPHICAL ABSTRACT

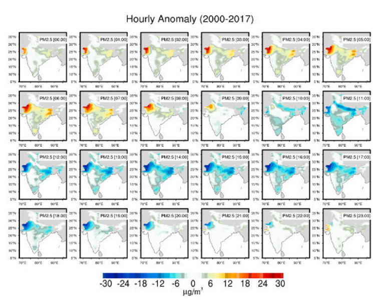

ARTICLE INFO

Keywords:
Ambient PM2.5
India
MERRA-2
Diurnal pattern
Dry-season

ABSTRACT

Modeling of ambient $PM_{2.5}$ exposure has improved in recent years with the application of satellite data, but in India, where the ground-based measurements are still inadequate, satellite-based assessment cannot provide temporal continuity. In this work, we analyze MERRA-2 (Modern-Era Retrospective analysis for Research and Applications) reanalysis aerosol products to estimate $PM_{2.5}$ at an hourly scale over India to fill the temporal sampling gap. MERRA-2 $PM_{2.5}$ calibrated using reference-grade monitors from the Central Pollution Control Board (CPCB) network show a statistically significant (at 95% CI) correlation ($r = 0.9$) against coincident in-situ measurements. Analyzing 18-years (2000–2017) data, we report the first detailed account of multi-year ambient $PM_{2.5}$ diurnal patterns in India. Diurnal amplitude is found to be quite large (>30 µg m^{-3}) in the Indo-Gangetic Basin (IGB) and western arid regions. We find a decrease in ambient $PM_{2.5}$ over the western dust source region and an increase over the parts of IGB and central India, primarily in the morning and evening hours. The annual trend is strongly governed by the trend during the dry season (October–February), attributed to a combination of the changing emission and meteorology. Our results suggest that the satellite-based exposure estimates that typically represent late morning to early afternoon hours are usually lower than the 24-h average exposure in most parts of India. Therefore, we call for the integration of reanalysis data that provide better temporal resolution with satellite data that provide better spatial resolution to further improve exposure estimates in data void regions like India for air quality studies.

* Corresponding author. Centre for Atmospheric Sciences, Indian Institute of Technology Delhi, Hauz Khas, New Delhi, India.
E-mail addresses: kunal.bali9@gmail.com (K. Bali), sagnik@cas.iitd.ac.in (S. Dey), dilipganguly@cas.iitd.ac.in (D. Ganguly).

https://doi.org/10.1016/j.atmosenv.2020.118180
Received 6 June 2020; Received in revised form 27 December 2020; Accepted 29 December 2020
Available online 31 December 2020

1. Introduction

Ambient $PM_{2.5}$ concentration is a leading health risk factor in the global burden of disease (Cohen et al., 2017). In India, 99% of the entire population is exposed to annual $PM_{2.5}$ exceeding the World Health Organization (WHO) annual air quality guideline of 10 $\mu g\ m^{-3}$. In 2017, nearly 77% of the Indian population exceeded the annual national ambient air quality standard (NAAQS) of 40 $\mu g\ m^{-3}$ (four times higher than the WHO AQG) with an estimated 0.67 (95% uncertainty interval [UI] 0.55–0.79) million premature death and an average loss of 0.9 (0.8–1.1) years of life expectancy (Balakrishnan et al., 2019). Ambient $PM_{2.5}$ exposure is further projected to increase in the future as India is expected to proliferate (Chowdhury et al., 2018; GBD MAPS Working Group, 2018). This prompted the Government of India to launch the National Clean Air Program (NCAP) in 2018. NCAP is about implementing an efficient air quality management plan to achieve sustainable development, for which the first step is a robust air quality monitoring system on a national scale.

India lacks an adequate ground-based network of $PM_{2.5}$ measurements (Brauer et al., 2019). Although $PM_{2.5}$ monitoring was started in India by the Central Pollution Control Board (CPCB) in 2008–2009, the network has expanded to around 200 continuous sites and 500+ manual sites that sample twice a week. India's current monitor density is much lower than that in China, where ambient $PM_{2.5}$ concentration was in the same range as India a few years ago but showed improvement in recent years (Zhao et al., 2018). Moreover, the monitoring sites are confined to urban areas leaving entire rural India unmonitored. To address this limitation in spatial coverage of $PM_{2.5}$ monitoring in India (and in many other developing countries), satellite aerosol optical depth (AOD) is used to infer $PM_{2.5}$. The methodology of converting satellite AOD to surface $PM_{2.5}$ evolved from a simple regression-based approach (Hoff et al., 2009) to a more complex chemical transport model-based (e.g., van Donkelaar et al., 2010, 2016; Brauer et al., 2015) and machine learning-based approach (e.g., Di et al., 2019; Murray et al., 2019). Such a satellite-based approach has been applied to generate $PM_{2.5}$ data for India (Dey et al., 2012; Chowdhury et al., 2016); however, satellite-based estimates typically represent the time when the passive sensors fly onboard polar satellites (e.g., Terra and Aqua) over a particular region. The existing sensors that provide robust AOD data are during the late morning to early afternoon hours. Furthermore, satellite AOD retrieval depends on the availability of cloud-free conditions, and hence AOD retrieval has data gaps, especially during the monsoon (June–September) season in India.

So far, four approaches have been adopted to address the temporal gap in sampling. First, AOD data from geostationary satellites allowed continuous $PM_{2.5}$ retrieval over a particular region throughout the day as long as the sunlight is available for AOD retrieval in cloud-free conditions (e.g., Chudnovsky et al., 2012; Lennartson et al., 2018). Even then, it is not possible to retrieve $PM_{2.5}$ estimates after sunset. Secondly, integrating $PM_{2.5}$ data from ground-based and satellite measurements in a Bayesian framework allowed filling the spatial and temporal gap in the concentration data (Shaddick et al., 2016; 2017). Thirdly, chemical transport modeling (CTM) can simulate $PM_{2.5}$ at an hourly scale (Michael et al., 2013). The accuracy of model-simulated $PM_{2.5}$ depends on the model physics, model configurations, and accuracy of the emission inventory (often not updated periodically). The fourth approach (Gui et al., 2020) is a machine learning technique that has been applied in China and a few places.

Here, we propose a fifth method to estimate the ambient $PM_{2.5}$ exposure diurnal pattern using reanalysis aerosol products. Reanalysis products generated by joint assimilation of meteorological and aerosol observations into global assimilation system take advantage of the best features of both observations and models (Randles et al., 2017) so that the space-time continuity in data is maintained with less uncertainty (Bocquet et al., 2015). We analyze 18-year (2000–2017) of reanalysis data at an hourly scale and present their climatology, trends, and the diurnal amplitude at a seasonal scale in India for the first time.

2. Data and methodology

2.1. MERRA-2 reanalysis dataset

We analyze MERRA-2 (Modern-Era Retrospective analysis for Research and Application) aerosol reanalysis data for this work generated by the GEOS-5 atmospheric model at $0.5^\circ \times 0.625^\circ$ horizontal resolution (Gelaro et al., 2017). A radiatively coupled version of the GOCART (Randles et al., 2016) model that considers the sources, sinks, and chemistry of 15 externally mixed aerosol species -dust in 5 size bins, sea-salt in 5 size bins, hydrophilic and hydrophobic organic carbon (OC) and black carbon (BC), and sulfate is used to generate MERRA-2 aerosol products (Randles et al., 2017). While emissions and transportations of dust and sea-salt are wind-driven, anthropogenic (EDGARv4.2) and biogenic sulfate (AeroCom Phase II) and carbonaceous aerosols (scaled RETROv2) are redistributed by winds after they are emitted (Lana et al., 2011). In the MERRA-2 dataset, the carbonaceous $PM_{2.5}$ is from biomass burning, anthropogenic sources, and plant matter (Buchard et al., 2017; Randles et al., 2017). Randles et al. (2017) and Buchard et al. (2017) also mentioned that Quick Fire Emissions Dataset (QFED) emission inventory (based on the MODIS fire radiative power) had been used from 2010 onward, but from the period of 1997–2009, the Global Fire Emission Dataset (GFEDv3.1) emission inventory has been introduced to simulate the aerosol emission from biomass burning in MERRA-2 reanalysis dataset (Darmenov and da Silva, 2013; Randerson et al., 2006; van der Werf et al., 2006). Some scaling factor was also introduced in the QFED to minimize the uncertainty among the biomass burning emission inventories (Buchard et al., 2017). Using two different inventories for different periods could also be responsible for the uncertainty in fire-based MERRA-2 $PM_{2.5}$.

MERRA-2 aerosol analysis assimilates quality-controlled AOD at 550 nm from four different sensors (MISR onboard Terra, MODIS onboard Terra and Aqua, AVHRR, and AERONET). Both the aerosol and meteorology observations are jointly assimilated in the GEOS-5 model. The AOD assimilation process includes the cloud screening and bias correction of spaces-based instruments (e.g., MODIS and AVHRR) with ground-based instrument AERONET. The GEOS-5 model also assimilates the non-biased corrected AOD from MISR (over the bright surface). GEOS-5 assimilates the real-time (for every 3 h) quality controlled AOD observation by using the local displacement ensemble (LDE) methodology (Buchard et al., 2016; 2017). LDE methodology is introduced to correct the misplaced aerosol plumes by considering the various aerosol properties such as speciation and vertical distribution of aerosols. On the other hand, in the regions where LDE is not applied, the AOD increment factor has been implemented, representing a vertical scaling factor; more detail can be found in Buchard et al., (2017).

In addition to this, Buchard et al. (2017) also performed some experiments with assimilation and without assimilation of AOD products over the global region. The results showed that aerosols with the assimilation system provide better estimates of surface $PM_{2.5}$ as they are well correlated with satellite-derived $PM_{2.5}$ from van Donkelaar et al. (2010). However, some discrepancies can be observed due to the lack of nitrate in the GOCART module and the low emission of OC (organic carbon) in the MERRA-2 dataset. The carbonaceous MERRA-2 $PM_{2.5}$ is mainly from biomass burning, anthropogenic sources, and plant matter (Buchard et al., 2017; Randles et al., 2017). Here, we assume that the contribution of OC concentration from biogenic sources is less because the aerosol emissions are mainly from biomass burning and anthropogenic sources in Northern India (Gani et al., 2019). More details of the MERRA-2 aerosol algorithm are provided in Randles et al. (2016), while extensive validation of the product is discussed in Buchard et al. (2017). The MERRA-2 reanalysis aerosol products are the hourly concentration of individual aerosol species smaller than 2.5 μm.

In our study, the MERRA-2 total $PM_{2.5}$ is estimated as

$$\text{MERRA-2 PM}_{2.5} = [\text{Dust}_{2.5}] + [\text{SS}_{2.5}] + [\text{BC}] + 1.6 \times [\text{OC}] + 1.375 \times [\text{SO}_4].$$

To obtain total $PM_{2.5}$, we simply add up dust and sea-salt in size bins smaller than 2.5 μm, hydrophilic and hydrophobic OC and BC, and sulfate, assuming their entire load within $PM_{2.5}$. Sulfate concentration is present in the form of neutralized ammonium sulfate $[(NH_4)_2SO_4]$ in MERRA-2 datasets, so a factor of 1.375 (Buchard et al., 2016; Song et al., 2018) is used to obtain the 'true' sulfate concentration. Organic carbon (OC) can be converted to particulate organic matter (POM) by a factor in the range 1.2–2.6 (Buchard et al., 2016; Malm et al., 2011) to account for contributions from other elements associated with other organic matter. We use the factor 1.6, which is more representative of the Indian region (Ram et al., 2012; Dey et al., 2020).

2.2. CPCB in-situ dataset

CPCB is the regulatory organization under the Ministry of Environment, Forest and Climate Change, Government of India, responsible for environmental management. CPCB launched a national air quality monitoring program (NAMP) to measure air pollution data of $PM_{2.5}$ using gravimetric (manual) measurement from 2008 to 2009. The NAAQS for the Indian region in 2009 was set as 60 μg m^{-3} for 24-h and 40 μg m^{-3} for annual concentration, which is higher than the WHO guideline of 25 μg m^{-3} for 24-h and 10 μg m^{-3} for annual concentration (Pant et al., 2018). CPCB also established a network with Continuous Automatic Air Quality Monitoring Station (CAAQMS) throughout major cities (with population > 1 million) in India. CPCB stations are generally installed in residential and industrial locations in urban areas (Gordon et al., 2018).

CPCB has adopted World Meteorological Organization protocols for sampling procedures, measurement methods, and quality control of the reference-grade data (CPCB, 2003; 2011). We analyze quality-controlled data from 75 sites (see Table S1 and Fig. S1 in SI for their locations) for 2009–2017. We note that the length of the data varies across the sites. We only process the data at an hourly scale to temporally match the hourly MERRA-2 data for the grids that contain at least one CPCB site.

2.3. Calibration and evaluation of MERRA-2 $PM_{2.5}$ with CPCB data

The diurnal variation in MERRA-2 data is primarily due to the changes in meteorology, as the emission data is not available at an hourly scale. Hence, we calibrate hourly MERRA-2 $PM_{2.5}$ with coincident $PM_{2.5}$ data (total sampling size>450,000) to reduce the low bias in MERRA-2 data reported by Navinya et al. (2020). We downscale MERRA-2 data using the bilinear interpolation technique. We adopt a percentile-based regression approach, where the bias in every 10th percentile of MERRA-2 $PM_{2.5}$ is estimated (Fig. 1a). Then we adjust hourly MERRA-2 data with the calibration factors of the respective percentile ranges.

Calibrated MERRA-2 data (Fig. 1b) show an increase in correlation coefficient and a decrease in root mean square error after the bias correction at every hour. The correlation coefficients are statistically significant at 95% CI ($p < 0.05$). We note that MERRA-2 $PM_{2.5}$ continues to underestimate at very high concentrations (i.e.,>300 μg m^{-3}). The flow-chart of the bias correction is shown in Fig. S2.

In terms of the spatial distribution of the bias (Fig. 2), a high bias (the difference between before and after bias correction) ~20 ± 3 μg/m^3 is observed over the IGP and low biases around ~5–10 μg/m^3 and ~12 μg/m^3 observed over the Jammu and Kashmir and rest of the Indian region respectively. The bias is higher during the nighttime and early morning than in the daytime, perhaps because satellite data assimilated in MERRA-2 do not retrieve aerosols at nighttime. The spatial climatology of hourly $PM_{2.5}$ before and after the bias correction at an annual scale is shown in Fig. S3.

We also compare the diurnal variation of $PM_{2.5}$ in each season – post-monsoon (Oct–Dec, OND), winter (Jan–Feb, JF), pre-monsoon (Mar–May, MAM) and monsoon (Jun–Sep, JJAS) from uncalibrated and calibrated MERRA-2 with CPCB data (Fig. 3). The black, blue, and red lines represent the mean of all 75 stations (2009–2017) from CPCB, uncalibrated MERRA-2, and calibrated MERRA-2, respectively.

Two observations are notable. Firstly, calibrated MERRA-2 $PM_{2.5}$ is much closer to CPCB data than the uncalibrated MERRA-2 data across a 24-hr period. Secondly, the calibrated MERRA-2 $PM_{2.5}$ can mimic the observed diurnal pattern in all the seasons; however, the bias remains low in the winter season. Capturing extreme pollution levels and a very shallow boundary layer is always challenging for the models. Nonetheless, MERRA-2 captures the variation of high (i.e., early morning or late evening) and low $PM_{2.5}$ concentration (noontime to 4 p.m.). Potential factors for the observed low bias in the winter could be lack of nitrate and underestimation of OC aerosol species in the GOCART module (Randles et al., 2016; Song et al., 2018) and bias in the simulation of panetary boundary layer (PBL) height in the GEOS-5 model. According to Rienecker et al. (2011), two types of schemes are introduced in the GEOS-5 model for simulating the atmospheric boundary layer in the MERRA-2 reanalysis dataset. The first scheme (Louis et al.,

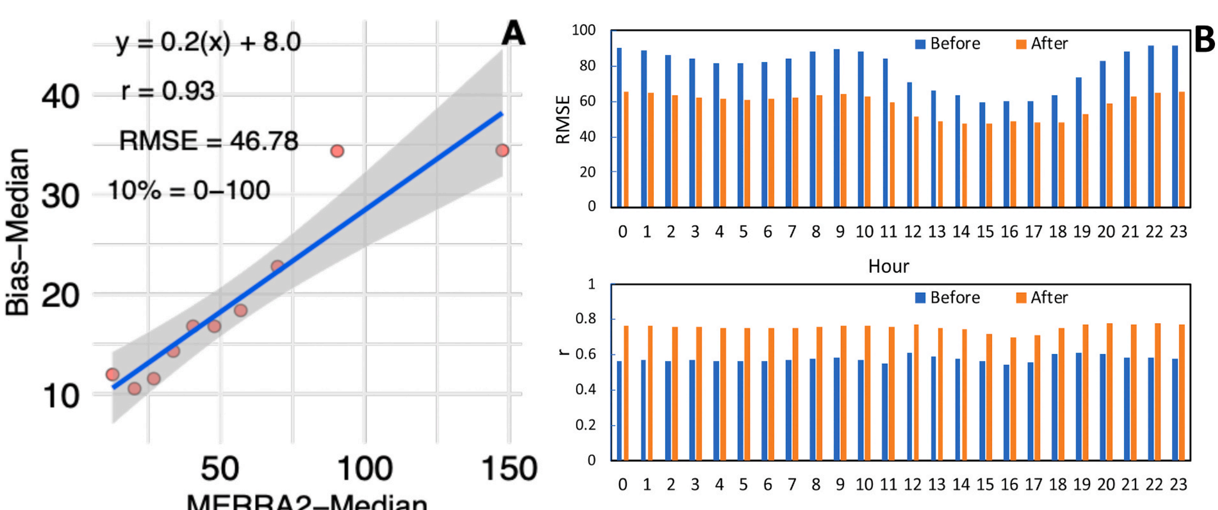

Fig. 1. Relationship between (a) the median bias in MERRA-2 data at every 10th percentile range and (b) the root mean square error (top panel) and correlation coefficient (bottom panel) at every hour before and after the bias correction. Spatio-temporal matching is done by averaging data from all ground-based monitoring sites falling within a single MERRA-2 grid for a 1-hr duration. A flow chart regarding data processing is given in supplementary information S2.

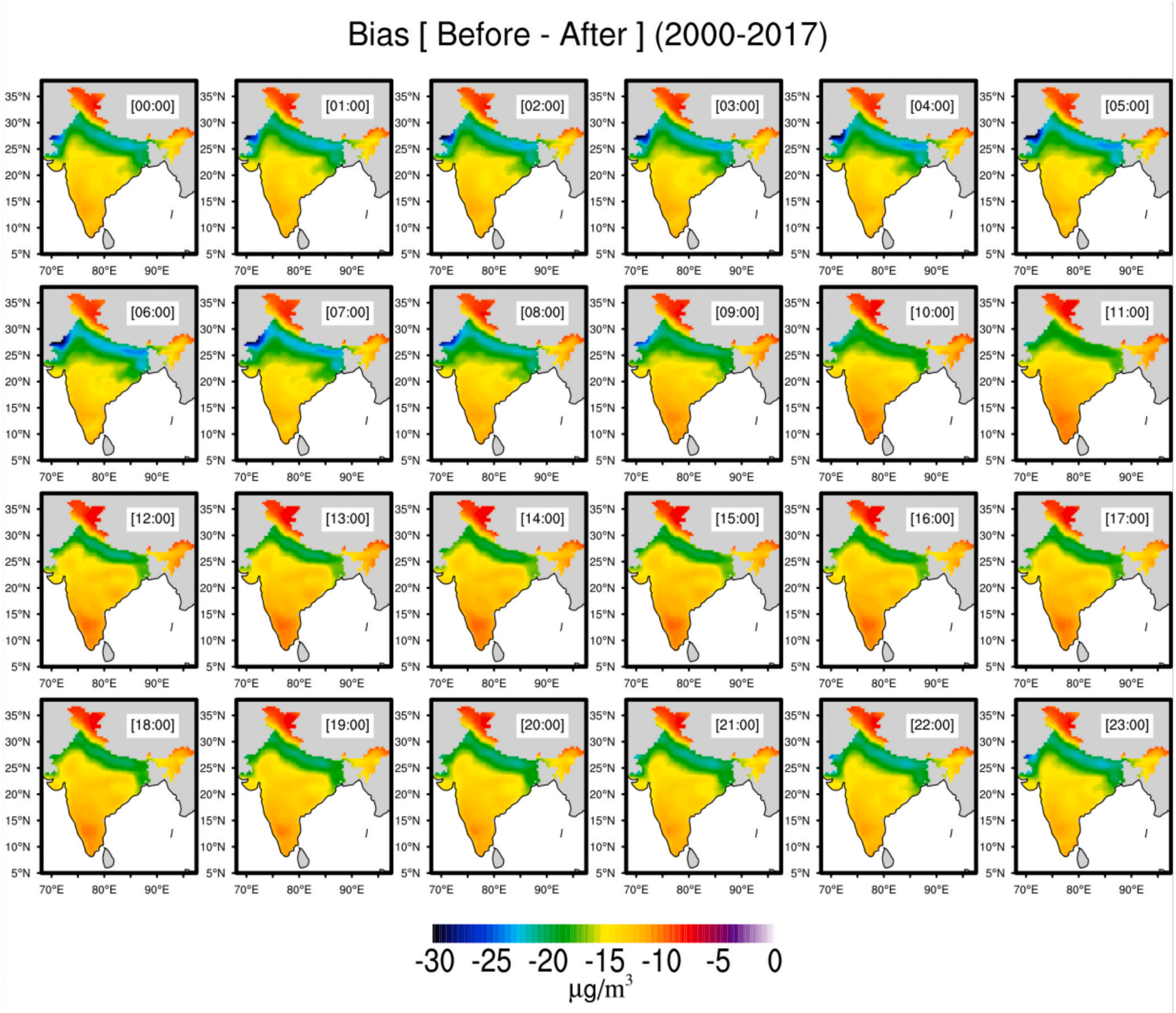

Fig. 2. Spatial variation of biases of hourly MERRA-2 $PM_{2.5}$ climatology for the period of 2000–2017.

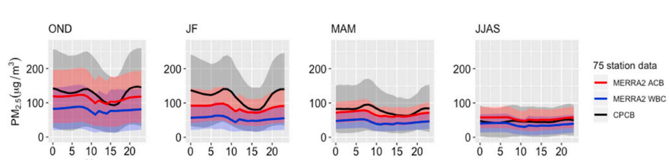

Fig. 3. Diurnal variation of $PM_{2.5}$ of CPCB, uncalibrated MERRA-2 (without bias correction, WBC), and calibrated MERRA-2 (after correcting bias, ACB) for OND, JF, MAM, and JJAS seasons. The shaded regions represent $\pm 1\sigma$ around seasonal mean across India.

1982) is based on the stable planetary condition in which no planetary boundary layer of clouds involved. The second scheme (Lock et al., 2000) is based on the unstable or cloud-topped planetary boundary layer conditions. Additionally, the GEOS-5 model uses two more schemes based on orographic conditions, such as orographic gravity wave drag (McFarlane 1987) and non-orographic waves (Garcia and Boville 1994). Such high levels of $PM_{2.5}$ exposure are episode-specific, and given the fact that most of the country does not have any ground-based monitoring, we proceed with the calibrated MERRA-2 $PM_{2.5}$ to examine the diurnal pattern over India.

Climatology for hourly ambient MERRA-2 $PM_{2.5}$ exposure (hereafter, we only refer to calibrated $PM_{2.5}$) is estimated by averaging $PM_{2.5}$ for that particular hour each day over the 18 years. Trends are computed using linear regression over the 18 years. Diurnal amplitude is estimated as the difference between the maximum and minimum $PM_{2.5}$ in each 24-h cycle, which is then averaged over the desired timescale to estimate the climatology. We identify the timing of the maximum and minimum $PM_{2.5}$ within a 24-h duration in each season to understand the diurnal pattern of ambient $PM_{2.5}$ concentration in India over the last 18 years.

2.4. Analysis of the meteorological data

MERRA PBL heights are diagnosed by the turbulence parameterization in the atmospheric general circulation model, based on the eddy diffusivity coefficient for heat. The PBL height is diagnosed as the lowest level at which the diffusion coefficients drop below a value of 1 m^2/s. Various meteorological variables (temperature, wind, and humidity) were introduced in the GEOS-5 model to assimilate the PBL heights. Regarding the performance of the GEOS-5 model for PBL height, Jordan et al. (2010) observed a good ($r = 0.7$) correlation of PBL height between CALIOP satellite and GEOS-5 model over the western hemisphere (e.g., American and African region). However, some disagreement was also observed over the equatorial Pacific Ocean, where GEOS-5 PBL height is lower than the CALIOP PBL height. In addition to PBL height, the other physical processes, such as aerosol mixing and hygroscopic growth, etc., could also contribute to the uncertainty in the aerosol model (Randles et al., 2016, Schutgen et al., 2010). We also analyze precipitation rate (PR) at the same hourly scale from MERRA-2 reanalysis data to understand their influence in modulating the observed diurnal pattern in ambient $PM_{2.5}$ exposure.

3. Results

3.1. Diurnal amplitude of ambient $PM_{2.5}$ exposure in India

Ambient $PM_{2.5}$ data from the ground-based sites (e.g., Apte et al., 2011; Goel et al., 2015) suggest a considerable variation in exposure within 24-hr. However, spatially limited in-situ data hinder in generating a regional picture. Satellite-based concentration estimates (van Donkelaar et al., 2010; Dey et al., 2012; Apte et al., 2015) assume that the concentration during satellite crossing time represents the 24 h. Hence, with large diurnal amplitude in $PM_{2.5}$ concentration, such estimates may have biases. Therefore, first, we report the spatial patterns of diurnal amplitude in ambient $PM_{2.5}$ exposure in India (Fig. 4).

During the post-monsoon and winter seasons (Oct–Feb), diurnal amplitude in ambient $PM_{2.5}$ exposure varies by $> 25\ \mu g\ m^{-3}$ in the entire Indo-Gangetic Basin (IGB), the western arid region that has been identified as a major dust source (Dey et al., 2012) and parts of northeast and south India. The pattern continues in Jan–Feb. In the rest of India, ambient $PM_{2.5}$ diurnal exposure varies by a smaller magnitude, while the amplitude exceeds 40 $\mu g\ m^{-3}$ in the eastern IGB states. In summer (Mar–May), the diurnal amplitude decreases in most parts of India except the arid regions, where it enhances further to $>50\ \mu g\ m^{-3}$. Overall, the least diurnal amplitude is observed in the monsoon (Jun–Sep) season.

To understand the observed diurnal amplitude's driving factors, we analyze the correlation between $PM_{2.5}$ and PBL height and PR (Fig. 5). As expected, PBL height and PR show a robust negative correlation with $PM_{2.5}$ concentration because deeper PBL facilitates pollution dispersion (Nakoudi et al., 2018), and large PR leads to washout of pollution. The arid region in western India barely receives rain large enough to influence $PM_{2.5}$ diurnal pattern, which can be attributed to the observed poor correlation ($r = -0.3$). In the high-altitude regions of the lower Himalayan belt and the Western Ghats, the pollution is lifted from the valley beneath as the PBL expands during the daytime, and therefore PBL height and $PM_{2.5}$ exposure is moderately correlated at an hourly scale (Srivastava et al., 2012).

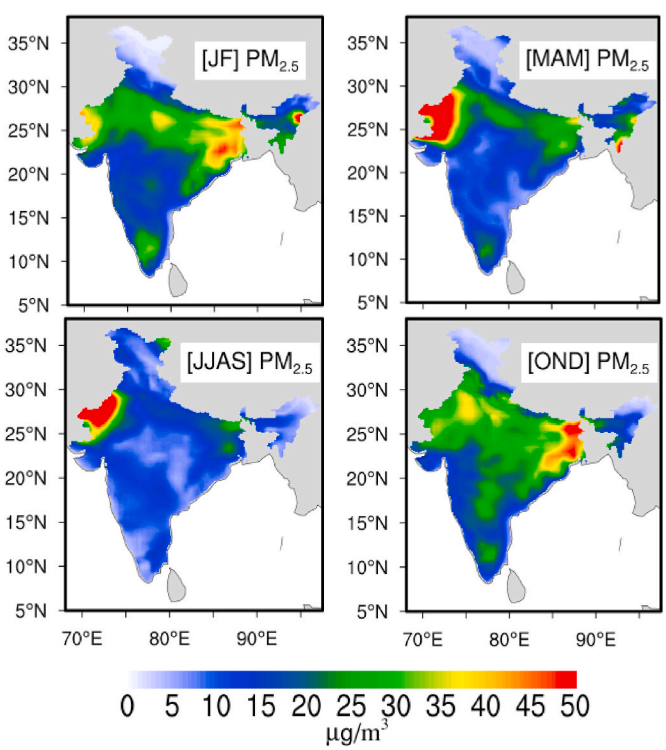

Fig. 4. Mean (over 18-years) seasonal, diurnal amplitude in ambient $PM_{2.5}$ concentration in India.

3.2. Timing of the maximum and minimum $PM_{2.5}$ exposure

We examine the seasonal shifts of the timings (in Indian standard time, IST) when $PM_{2.5}$ exposure is the highest and lowest within 24 h (Fig. 6). In large part of the country, ambient $PM_{2.5}$ exposure peaks around early morning hours (6–8 IST) during Oct–Feb. In the eastern part of the IGB and northeastern India, the peak hours are around midnight during these months, while in the northern hilly regions, peak hours are in the late afternoon to the early evening after the PBL fully evolves. The PBL expansion effect is not so prominent along with the Western and Eastern Ghat mountain ranges in these months but can be seen in the summer months. The lowest concentration is found during 13–15 IST in the post-monsoon season that gradually shifts to evening hours (16–20 IST) in most parts of the country during the winter. Similar timing (late afternoon) in the lowest $PM_{2.5}$ concentration is observed in central India, parts of north and south India during Mar–May that further shrinks to only a part of the west and central India during the monsoon season. During these months, the lowest $PM_{2.5}$ concentration is observed during 10–12 IST in the rest of the country.

3.3. Hourly climatology and trends of ambient $PM_{2.5}$ exposure

Spatial patterns of annual ambient $PM_{2.5}$ exposure at hourly scale in Fig. 7 (statistics at seasonal scale and the corresponding anomaly relative to 24-hr average are shown in the SI, Figs. S4–S11) reveals large ($>12\ \mu g\ m^{-3}$) positive anomaly relative to 24-hr average during the night and early morning hours over the arid regions in the west, IGB, and parts of peninsular India. Key notable features are as follows. North (high $PM_{2.5}$)-south (low $PM_{2.5}$) spatial gradient in $PM_{2.5}$ is maintained throughout the 24-h duration. Even during the noontime and afternoon hours when the ambient $PM_{2.5}$ exposure is at its minimum in most parts of India, it remains higher than the NAAQS in the IGB and western arid region. As discussed in the previous subsection, these two regions have

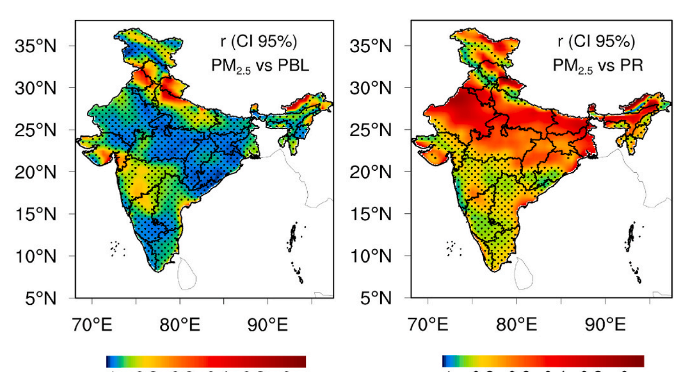

Fig. 5. Spatial distribution of correlation coefficients between ambient $PM_{2.5}$ concentration and (a) planetary boundary layer (PBL) and (b) precipitation rate (PR) with the hatched regions showing a 95% CI.

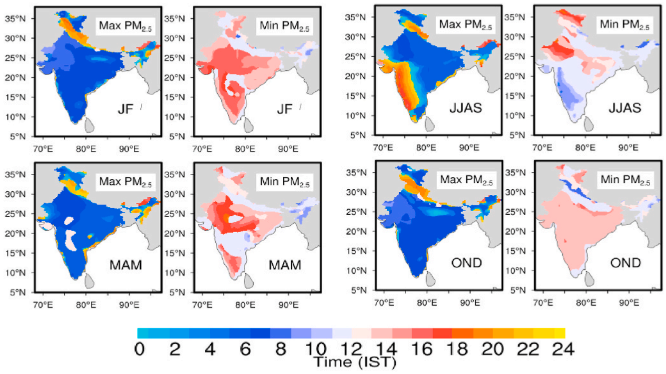

Fig. 6. Seasonal shifts in the timings of the maximum and minimum ambient $PM_{2.5}$ concentration in India.

the largest diurnal amplitude in $PM_{2.5}$ exposure throughout the year.

In Peninsular India, diurnal variation is less prominent at the annual scale though the magnitude varies from season to season (see SI). During Jan–Feb, ambient $PM_{2.5}$ exposure in India at 15–16 IST is the best representative of the 24-hr average. $PM_{2.5}$ exposure is higher than the 24-h average by $> 10\ \mu g\ m^{-3}$ in most parts of the country during the late evening to early morning hours, with higher values in the IGB from 22:00 to 04:00 IST. During the morning hours, $PM_{2.5}$ exposure decreases as the PBL expands. A similar diurnal pattern is observed during March–May and Oct–Dec but with a larger diurnal amplitude. In Jun–Sep, the diurnal variation is only prominent in the western arid region.

We further examine the annual trends of ambient $PM_{2.5}$ for every hour (Fig. 8). A positive trend over the 18 years is observed in most parts of India, with values exceeding 1 $\mu g\ m^{-3}$ per year in the Himalayan foothills, northeastern India, eastern IGB, and parts of western IGB. In most parts of the Indian regions, the observed positive trend at annual scale ($>2\ \mu g\ m^{-3}$ per year) is primarily governed by a massive increase during October–February (see Figs. S12–S15 for the trends at seasonal scale). Unfortunately, no available emission inventory captures anthropogenic emissions at an hourly scale. Along with the traditional anthropogenic pollution sources (e.g., household emission, vehicles, industries, construction activities, etc.), open burning of agricultural crop-waste and brick kilns adds to the dry season's emission. In a recent study (Dey et al., 2020), the trends in annual $PM_{2.5}$ averaged over 24-hr were observed to be higher over eastern and peninsular India than in the IGP. We also note that a part of this trend could be influenced by trends in satellite AODs assimilated into MERRA-2. However, AODs are retrieved at specific times, and hence, the observed trends at an hourly scale also depend on the model's ability to simulate the meteorology.

Trend analysis of PBL height (see Figs. S16–S19) suggests that PBL height is becoming shallower over the years in most parts of India during the dry season with a higher rate in the late afternoon to early morning hours. Usually, the anthropogenic activities peak during the morning hours and the emissions from specific sectors (e.g., vehicles, industries, construction, etc.) are expected to subside in the late evening-early morning hours. The combined effect is a nearly similar trend in $PM_{2.5}$ exposure in the dry season throughout the 24 h.

PBL height does not show any significant trend in the monsoon season, reflected in a negligible trend in $PM_{2.5}$ concentration (see Fig. S18). In the western arid regions during MAM and high-altitude areas throughout the year, PBL height shows an increasing trend. This increasing trend of PBL height, which facilitates dispersion of aerosols, is perhaps driving the decreasing trend of ambient $PM_{2.5}$ exposure (by $> 1.5\ \mu g\ m^{-3}$ per year) over the western arid region. This is consistent with the reported decline in dust transport in this region (Pandey et al., 2017). On the contrary, large PBL height in the high-altitude areas would allow the pollution to be lifted up from the valley beneath more efficiently. This could explain the increasing trend of $PM_{2.5}$ concentration in these regions during the dry season.

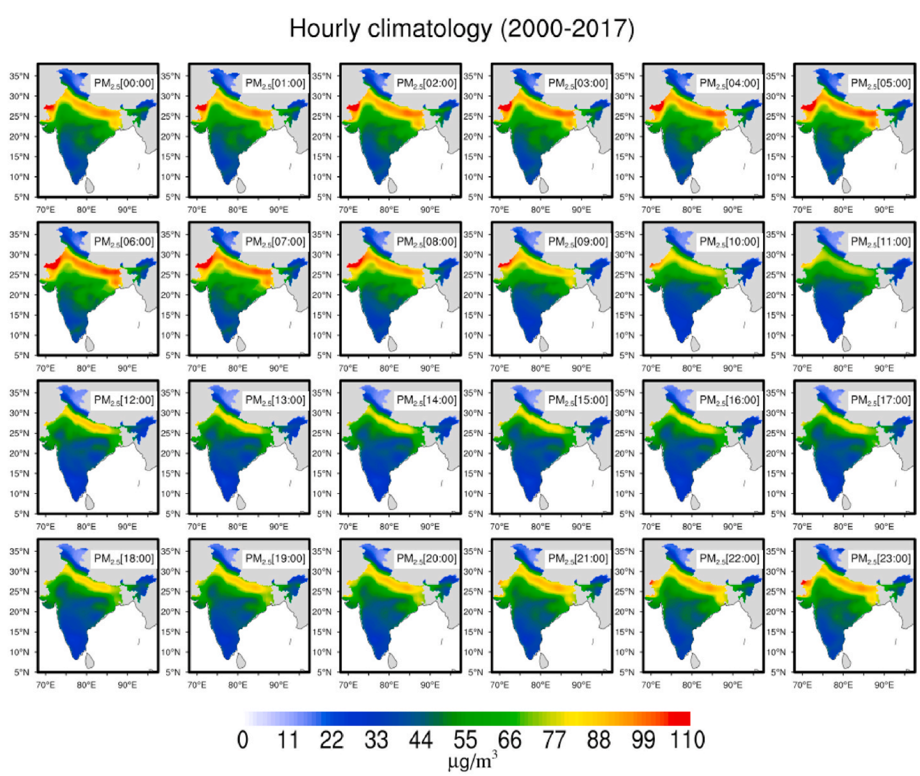

Fig. 7. Mean annual ambient $PM_{2.5}$ exposure in India for each hour cycle (00:00 IST represents 00:00–01:00 IST duration).

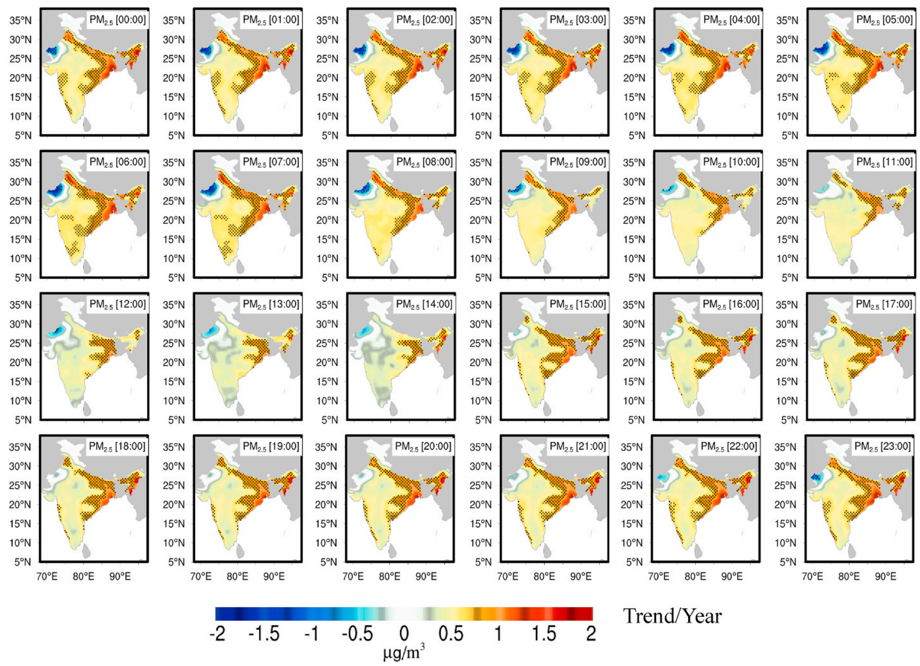

Fig. 8. Annual trends of ambient $PM_{2.5}$ exposure (with the hatched regions showing 95% CI) in India for each hour cycle during the day (00:00 IST represents 00:00–01:00 IST duration).

4. Discussion and conclusions

Previously, ambient $PM_{2.5}$ exposure in India has been estimated using either data from limited ground-based monitors (Tiwari et al., 2013) or satellites (van Donkelaar et al., 2010, 2016; Brauer et al., 2015; Dey et al., 2012; Chowdhury and Dey, 2016). Neither of them provides complete spatio-temporal coverage. Even the geostationary satellite-based AOD product (e.g., Mishra, 2018) is insufficient to provide 24-h coverage. In this work, we propose using MERRA-2 aerosol reanalysis data to resolve the temporal gap in the data. We map the hour-by-hour changes in $PM_{2.5}$ concentration over 18-year (2000–2017) period for the whole country. We note that our bias correction relies on the CPCB sites deployed in the urban locations and assumes that the patterns of the biases are more or less similar in the rural areas. Unless the ground-based monitoring network expands to the rural areas, this issue cannot be addressed fully. However, since the CPCB network covers a broad geographical region, we expect that the bias-corrected data would quite reasonably represent the regions.

Our results reveal a large diurnal amplitude in $PM_{2.5}$ exposure in some areas of India and identify the times of maximum and minimum exposure and its seasonal shift. This explains the underestimation in satellite-based $PM_{2.5}$ exposure estimates (related to ground-based measurements that cover 24-h duration) that uses AOD data from sensors onboard polar-orbiting satellites crossing India in the late morning to early afternoon hours. In the regions where the diurnal amplitude is small, satellite-based estimates of exposures are more representative. We also show that the increasing trend at the annual scale is strongly controlled by an increase in $PM_{2.5}$ during the Oct–Feb period. This suggests that if the emissions during these months can be controlled at the source, the increasing annual trend can be arrested.

The large increasing trend of $PM_{2.5}$ in the Himalayan foothills is a matter of concern as transport of pollution to the Himalayan region can adversely affect the cryosphere (Bali et al., 2017). Another key result is the declining trend in PBL height over a large part of India, especially during the dry season that might have played a major role in the observed increasing trend in $PM_{2.5}$ exposure. Shallow PBL leads to stagnation that entraps the pollutants closer to the surface, increasing $PM_{2.5}$ concentration and therefore, exposure. Under global warming, stagnation events are projected to increase in the future over India (Horton et al., 2014). Therefore, cutting down emissions at the source seems to be the only sustainable solution in addressing India's air pollution problem.

Although we map hour-by-hour changes in $PM_{2.5}$ concentration in this work, we cannot identify the primary sources with this data alone. Further analysis is required to attribute source characterization to the observed hourly variation in $PM_{2.5}$ exposure. However, this study provides the opportunity to identify the major sources that can be attributed to the maximum $PM_{2.5}$ (corresponding to the observed peak timing) exposure at a regional scale.

The integration of the spatially and temporally continuous MERRA-2 reanalysis data with ground-based measurements (temporally continuous) and satellite-based measurements (temporally discontinuous but can provide information at high spatial resolution) is perhaps the way forward in the future. We hope these results would help formulate better air pollution mitigation plans so that the national burden of disease attributed to ambient air pollution could be decreased by evidence-based policy actions at the regional and national levels.

CRediT authorship contribution statement

Kunal Bali: Formal analysis, Writing - original draft. **Sagnik Dey:** Conceptualization. **Dilip Ganguly:** interpretation.

Declaration of competing interest

The authors declare that they have no known competing financial interests or personal relationships that could have appeared to influence the work reported in this paper.

Acknowledgments

The authors acknowledge financial support from the Ministry of Environment, Forest and Climate Change, Govt. Of India through a research grant (No. 14/10/2014-CC) under the NCAP-COALESCE project. The authors thank the internal review committee of the NCAP-COALESCE project for their comments and suggestions. The views expressed in this document are solely those of authors and do not necessarily reflect those of the Ministry. SD acknowledges financial support from the Central Pollution Control Board through a research grant No. B-12015/101/2019-AS/205 and from IIT Delhi for the Institute Chair position. MERRA-2 reanalysis datasets are provided by NASA. The authors acknowledge Neetu Singh for helping in downloading all CPCB data. The authors acknowledge the DST-FIST grant (SR/FST/ESII-016/2014) for computing support.

Appendix A. Supplementary data

Supplementary data to this article can be found online at https://doi.org/10.1016/j.atmosenv.2020.118180.

References

Apte, J.S., Kirchstetter, T.W., Reich, A.H., Deshpande, S.J., Kaushik, G., Chel, A., Marshall, J.D., Nazaroff, W.W., 2011. Concentrations of fine, ultrafine, and black carbon particles in auto-rickshaws in New Delhi, India, Atmos. Environ. Times 45, 4470–4480.

Apte, J.S., Marshall, J.D., Cohen, A.J., Brauer, M., 2015. Addressing global mortality from ambient $PM_{2.5}$. Environ. Sci. Technol. 49, 8057–8066.

Balakrishnan, K., Dey, S., Gupta, T., et al., 2019. The impact of air pollution on deaths, disease burden, and life expectancy across the states of India: the Global Burden of Disease Study 2017. The Lancet Planetary Health 3, 26–39.

Bali, K., Mishra, A.K., Singh, S., 2017. Impact of anomalous forest fire on aerosol radiative forcing and snow cover over Himalayan region. Atmos. Environ. 150, 264–275.

Brauer, M., Freedman, G., Frostad, J., Van Donkelaar, A., Martin, R.V., Dentener, F., Dingenen, R.V., Estep, K., Amini, H., Apte, J.S., Balakrishnan, K., 2015. Ambient air pollution concentration estimation for the global burden of disease 2013. Environ. Sci. Technol. 50, 79–88.

Brauer, M., Guttikunda, S.K., Nishad, K.A., Dey, S., Tripathi, S.N., Weagle, C., Martin, R.V., 2019. Examination of Monitoring approaches for air pollution in India. Atmos. Environ. 216.

Bocquet, M., et al., 2015. Data assimilation in atmospheric chemistry models: current status and future prospects for coupled chemistry meteorology models. Atmos. Chem. Phys. 15, 5325–5358.

Buchard, V., da Silva, A.M., Randles, C.A., Colarco, P., Ferrare, R., Hair, J., Hostetler, C., Tackett, J., Winker, D., 2016. Evaluation of the surface PM2.5 in version 1 of the NASA MERRA aerosol reanalysis over the United States. Atmos. Environ. 125, 100–111.

Buchard, V., Randles, C.A., da Silva, A.M., Darmenov, A., Colarco, P.R., Govindaraju, R., Ferrare, R., Hair, J., Beyersdorf, A.J., Ziemba, L.D., Yu, H., 2017. The MERRA-2 aerosol reanalysis, 1980 onward. Part II: evaluation and case studies. J. Clim. 30, 6851–6872.

Central Pollution Control Board (CPCB), 2003a. Guidelines for ambient air quality monitoring; series: NAAQMS/.../2003-04. Central Pollution Control Board. https://tinyurl.com/y8r54a3z.

Central Pollution Control Board (CPCB), 2011. Guidelines for the measurement of ambient air pollutants volume-II. Central Pollution Control Board. https://tinyurl.com/ycjs4h8j.

Central Pollution Control Board (CPCB), 2003b. Ambient Air Quality Statistics for Indian Metro Cities. Central Pollution Control Board, Zonal Office, Bangalore.

Chowdhury, S., Dey, S., Smith, K.R., 2018. Ambient $PM_{2.5}$ concentration and expected premature mortality to 2100 in India under climate change scenarios. Nat. Commun. 9, 318.

Chowdhury, S., Dey, S., 2016. Cause-specific premature death from ambient PM2.5 concentration in India: estimate adjusted for baseline mortality. Environ. Int. 91, 283–290.

Chudnovsky, A.A., Lee, H.J., Kostinski, A., Kotlov, T., Koutrakis, P., 2012. Prediction of daily fine particulate matter concentrations using aerosol optical depth retrievals from the Geostationary Operational Environmental Satellite (GOES). J. Air Waste Manag. Assoc. 62, 1022–1031.

Cohen, A.J., Brauer, M., Burnett, R., et al., 2017. Estimates and 25-year trends of the global burden of disease attributable to ambient air pollution: an analysis of data from the Global Burden of Diseases Study 2015. Lancet 389, 1907–1918.

Darmenov, A., da Silva, A., 2013. The quickfire emissions dataset (QFED)–documentation of versions 2.1, 2.2 and 2.4. NASA technical report series on global modeling and data assimilation. NASA TM-2013-104606 32, 83.

Dey, S., Di Girolamo, L., van Donkelaar, A., Tripathi, S.N., Gupta, T., Mohan, M., 2012. Variability of outdoor fine particulate ($PM_{2.5}$) concentration in the Indian Subcontinent: a remote sensing approach. Rem. Sens. Environ. 127, 153–161.

Di, Q., et al., 2019. An ensemble-based model of $PM_{2.5}$ concentration across the contiguous United States with spatio-temporal resolution. Environ. Int. 130, 104909.

GBD MAPS Working Group, 2018. Burden of Disease Attributable to Major Air Pollution Sources in India. Special Report, vol. 21. Health Effects Institute, Boston, MA.

Gani, S., Bhandari, S., Seraj, S., Wang, D.S., Patel, K., Soni, P., Arub, Z., Habib, G., Hildebrandt Ruiz, L., Apte, J.S., 2019. Submicron aerosol composition in the world's most polluted megacity: the Delhi Aerosol Supersite study. Atmos. Chem. Phys. 19, 6843–6859.

Gelaro, R., McCarty, W., Suárez, M.J., Todling, R., Molod, A., Takacs, L., Randles, C.A., Darmenov, A., Bosilovich, M.G., Reichle, R., Wargan, K., 2017. The modern-era retrospective analysis for research and applications, version 2 (MERRA-2). J. Clim. 30, 5419–5454.

Goel, R., Gani, S., Guttikunda, S.K., Wilson, D., Tiwari, G., 2015. On-road PM2. 5 pollution concentration in multiple transport microenvironments in Delhi, Atmos. Environ. Times 123, 129–138.

Garcia, R.R., Boville, B.A., 1994. Downward control of the mean meridional circulation and temperature distribution of the polar winter stratosphere. J. Atmos. Sci. 51, 2238–2245.

Gui, K., Che, H., Zeng, Z., Wang, Y., Zhai, S., Wang, Z., Luo, M., Zhang, L., Liao, T., Zhao, H., Li, L., 2020. Construction of a virtual PM2. 5 observation network in China based on high-density surface meteorological observations using the Extreme Gradient Boosting model. Environ. Int. 141, 105801.

Hoff, R.M., Christopher, S.A., 2009. Remote sensing of particulate pollution from space: have we reached the promised land? J. Air Waste Manag. Assoc. 59, 645–675.

Horton, D.E., Skinner, C.B., Singh, D., Diffenbaugh, N.S., 2014. Occurrence and persistence of future atmospheric stagnation events. Nat. Clim. Change 4, 698.

Jordan, N.S., Hoff, R.M., Bacmeister, J.T., 2010. Validation of Goddard Earth Observing System-version 5 MERRA planetary boundary layer heights using CALIPSO. J. Geophys. Res. 115.

Lennartson, E.M., Wang, J., Gu, J., Castro Garcia, L., Ge, C., Gao, M., Choi, M., Saide, P. E., Carmichael, G.R., Kim, J., Janz, S.J., 2018. Diurnal variation of aerosol optical depth and PM 2.5 in South Korea: a synthesis from AERONET, satellite (GOCI), KORUS-AQ observation, and the WRF-Chem model. Atmos. Chem. Phys. 18, 15125–15144.

McFarlane, N.A., 1987. The effect of orographically excited gravity wave drag on the general circulation of the lower stratosphere and troposphere. J. Atmos. Sci. 44, 1775–1800.

Mishra, M.K., 2018. Retrieval of aerosol optical depth from INSAT-3D imager over asian landmass and adjoining ocean: retrieval uncertainty and validation. J. Geophy. Res. Atmos. 123, 5484–5508.

Murray, N.L., Holmes, H.A., Liu, Y., Chang, H.H., 2019. Bayesian ensemble approach to combine $PM_{2.5}$ estimates from statistical models using satellite imagery and numerical model simulation. Environ. Res. 178, 108601.

Nakoudi, K., Giannakaki, E., Dandou, A., Tombrou, M., Komppula, M., 2018. Planetary boundary layer variability over New Delhi, India, during EUCAARI project. Atmos. Meas. Tech. Discuss. 20, 809.

Navinya, C.D., Vinoj, V., Pandey, S.K., 2020. Evaluation of $PM_{2.5}$ surface concentrations simulated y NASA's MERRA Version 2 aerosol reanalysis over India and its relation to the air quality index. Aero. Air Qual. Res. 20, 1329–1339.

Pandey, S., Vinoj, V., Landu, K., Suresh Babu, S., 2017. Declining pre-monsoon dust loading over South Asia: signature of a changing regional climate. Sci. Rep. 7, 16062, 2017.

Ram, K., Sarin, M.M., Tripathi, S.N., 2012. Temporal trends in atmospheric PM2. 5, PM10, elemental carbon, organic carbon, water-soluble organic carbon, and optical properties: impact of biomass burning emissions in the Indo-Gangetic Plain. Environ. Sci. Technol. 46, 686–695.

Randles, C.A., Da Silva, A.M., Buchard, V., Colarco, P.R., Darmenov, A., Govindaraju, R., Smirnov, A., Holben, B., Ferrare, R., Hair, J., Shinozuka, Y., 2017. The MERRA-2 aerosol reanalysis, 1980 onward. Part I, System description and data assimilation evaluation. J. Clim. 30, 6823–6850.

Randles, C.A., Da Silva, A.M., Buchard, V., Darmenov, A., Colarco, P.R., Aquila, V., Bian, H., Nowottnick, E.P., Pan, X., Smirnov, A., Yu, H., Govindaraju, R., 2016. The MERRA-2 aerosol assimilation. Technical report series on global modeling and data assimilation 44, NASA global modeling and assimilation office. available online at: https://gmao.gsfc.nasa.gov/reanalysis/MERRA-2/docs/.

Song, Z., Fu, D., Zhang, X., Wu, Y., Xia, X., He, J., Han, X., Zhang, R., Che, H., 2018. Diurnal and seasonal variability of $PM_{2.5}$ and AOD in North China plain: comparison of MERRA-2 products and ground measurements. Atmos. Environ. 191, 70–78.

Srivastava, A.K., Singh, S., Pant, P., Dumka, U.C., 2012. Characteristics of black carbon over Delhi and Manora Peak—a comparative study. Atmos. Sci. Lett. 13, 223–230.

Tiwari, S., Srivastava, A.K., Bisht, D.S., Parmita, P., Srivastava, M.K., Attri, S.D., 2013. Diurnal and seasonal variations of black carbon and $PM_{2.5}$ over New Delhi, India: influence of meteorology. Atmos. Res. 125, 50–62.

van Donkelaar, A., Martin, R.V., Brauer, M., Kahn, R., Levy, R., Verduzco, C., Villeneuve, P.J., 2010. Global estimates of ambient fine particulate matter concentrations from satellite-based aerosol optical depth: development and application. Environ. Health Perspect. 118, 847–855.

van Donkelaar, A., Martin, R.V., Brauer, M., Hsu, N.C., Kahn, R.A., Levy, R.C., Lyapustin, A., Sayer, A.M., Winker, D.M., 2016. Global estimates of fine particulate matter using a combined geophysical-statistical method with information from satellites, models, and monitors. Environ. Sci. Technol. 50, 3762–3772.

Zhao, B., Zheng, H., Wang, S., Smith, K.R., Lu, X., Aunan, K., Gu, Y., Wang, Y., Ding, D., Xing, J., Fu, X., 2018. Change in household fuels dominates the decrease in PM2. 5 exposure and premature mortality in China in 2005–2015. Proc. Natl. Acad. Sci. Unit. States Am. 115 (49), 12401–12406.